Acta Cryst. (1977). B**33**, 2175–2181

The Crystal Structure of a Lithium–Nickel Molybdate, $Li_2Ni_2Mo_3O_{12}$, and the Systematics of the Structure Type

BY M. OZIMA AND S. SATO

Institute for Solid State Physics, University of Tokyo, Roppongi-7, Minato-ku, Tokyo 106, *Japan*

AND T. ZOLTAI

Department of Geology and Geophysics, University of Minnesota, Minneapolis, Minnesota 55455, *USA*

(*Received* 2 *December* 1976; *accepted* 24 *December* 1976)

$Li_2Ni_2Mo_3O_{12}$ is orthorhombic, $a = 10{\cdot}423$ (3), $b = 17{\cdot}525$ (4), $c = 5{\cdot}074$ (1) Å, space group *Pmcn* with $Z = 4$. 2717 independent reflexions were collected and the structure was refined to an R value of 0·053. The average Mo–O and (Ni,Li)–O distances are 1·774 and 2·097 Å, respectively. The close-packed sheets of O are composed of three-square-wide bands of Wells's No. 9 regular net, held together by semi-regular single chains of triangles. There are two identical sheets in the stacking sequence, and the regular and semi-regular voids between the O atoms are filled by the cations: Ni and Li occupy, in various proportions, the trigonal prism (*M*1), the distorted (*M*2) and the regular (*M*3) trigonal antiprisms, and Mo occupies the elongated tetrahedral voids.

Experimental

Single crystals of $Li_2Ni_2Mo_3O_{12}$ were produced accidentally during an attempt to grow nickel-olivine crystals by a flux method (Ozima & Zoltai, 1976). One of these crystals, 0·07 × 0·07 × 0·08 mm, was mounted on an automated, four-circle Rigaku diffractometer and three-dimensional intensities were collected with Mo $K\alpha$ radiation, monochromated by a graphite plate. The intensities of the reflexions were collected in the ω–2θ mode. The intensities of three standard reflexions were checked after every 50 measurements. 2980 independent intensities were collected up to $2\theta = 80°$. Of these, 2717 intensities were sufficiently strong for consideration. All intensities were corrected for Lorentz and polarization effects, but no corrections were made for primary and secondary extinction, or for absorption. The last appeared to be unnecessary as the crystal was almost an equidimensional cube.

The unit-cell parameters were calculated and refined by a least-squares analysis of the 2θ values of 38 high-angle reflexions. The unit translations obtained are: $a = 10{\cdot}423$ (3), $b = 17{\cdot}525$ (4) and $c = 5{\cdot}074$ (1) Å.

Other crystallographic data determined and calculated are: space group *Pmcn* (No. 62), $Z = 4$, $D_x = 4{\cdot}372$, $D_m = 4{\cdot}36$ g cm^{-3}, $\mu_c = 83{\cdot}5$ cm^{-1} for Mo $K\alpha$ ($\lambda = 0{\cdot}7107$ Å) radiation.

Structure determination and refinement

Three-dimensional Patterson maps were computed and were solved for the Mo and Ni atomic coordinates by recognition of the vectors of these relatively heavy atoms. The locations of the O and Li atoms were obtained from a Fourier difference synthesis. The structure was subsequently refined by minimizing $\Sigma\,(|F_o| - |F_c|)^2$ through full-matrix least-squares calculations based on the 2717 observed intensities. Anisotropic thermal parameters for Mo, Ni and O and isotropic thermal parameters for Li were also calculated. The final R value obtained was 0·053. The atomic coordinates are given in Table 1.

The Ni–Li distribution pattern in *M*1, *M*2 and *M*3 sites was also determined. The *M*1 site is occupied by Li and the *M*2 and *M*3 sites by Ni and Li in the ratio Ni : Li 0·731 : 0·269 and 0·538 : 0·462 respectively.

The analysis of the list of observed and calculated

Table 1. *Atomic coordinates* (×10^4)

	x	*y*	*z*
Mo(1)	7500	0565 (0)	7158 (1)
Mo(2)	4738 (0)	1564 (0)	2211 (1)
*M*2-Ni	4284 (1)	0265 (1)	7475 (2)
*M*3-Ni	7500	2506 (1)	3919 (4)
O(1)	2500	0065 (4)	5632 (12)
O(2)	7500	1544 (3)	6358 (12)
O(3)	6176 (4)	2048 (2)	1400 (8)
O(4)	3774 (5)	2135 (3)	4202 (10)
O(5)	3866 (4)	1255 (2)	9403 (9)
O(6)	5122 (4)	0745 (2)	4207 (8)
O(7)	6148 (4)	0363 (2)	9185 (8)
*M*1-Li	2500	1951 (10)	5568 (43)
*M*2-Li	4284	0265	7475
*M*3-Li	7500	2506	3919

structure factors* indicates that there is probably a small extinction effect in the observed intensities. Some of the observed, strong reflexions have lower F values than their calculated equivalents.

The scattering factors for Mo^{6+}, Ni^{2+}, Li^{+} and anomalous dispersion corrections for Mo and Ni were taken from *International Tables for X-ray Crystallography* (1974). The scattering factor for O^{2-} given by Tokonami (1965) was used.

Description of the structure

The structure of $Li_2Ni_2Mo_3O_{12}$ is unusual but not unique. It is virtually identical with the structures of $NaCo_{2.31}Mo_3O_{12}$ (Ibers & Smith, 1964), $Li_3Fe^{3+}Mo_3O_{12}$ and $Li_2Fe_2^{2+}Mo_3O_{12}$ (Klevtsova & Magarill, 1971), and is comparable with the structure of $Cu_4Mo_3O_{12}$ (Katz, Kasenally & Kihlborg, 1971). This structure type is usually interpreted as being composed of four different coordination polyhedral elements:

(1) $M1$ (Li) trigonal prisms form single chains by sharing edges as shown in Fig. 1(*a*). These chains provide the connexion between $M2$ layers and are parallel with the octahedral (or antiprismatic) chains of $M3$. In $Cu_4Mo_3O_{12}$, the trigonal prism is changed to a distorted tetragonal pyramid that results in fivefold coordination similar to that found in some Cu compounds. The tetragonal pyramids, like the trigonal prisms, form chains.

(2) $M2$ (Li,Ni,Co,Cu,Fe) distorted octahedra (or antiprisms) constitute an indented and incomplete layer in the (010) plane (see Fig. 2). This layer is composed of single chains of edge- and corner-sharing distorted octahedra, with two octahedra per repeat unit. Mirror equivalents of these chains across (100), are joined through sharing of one O per octahedra on alternating sides. The chains are oriented in the (001) direction and the indentation of the layers is the consequence of two perpendicular directions of corrugation, the (100) and (001) directions.

(3) $M3$ (Li,Ni,Co,Cu,Fe) face-sharing octahedral (or antiprismatic) chains (see Fig. 1*b*) are in the centre of the large channels in the three-dimensional network of the $M2$ octahedral layers and the $M1$ chains. These columns of octahedra are not linked to either the $M2$ layers or the $M1$ chains.

(4) Mo tetrahedra provide the attachment of the $M3$ chains to the $M1$–$M2$ network. There are two nonequivalent tetrahedra: $T1$ shares three corners with two $M2$ distorted octahedra, one corner with two $M3$ octahedra; $T2$ shares one corner with two $M3$ octahedra,

* Lists of structure factors and thermal parameters have been deposited with the British Library Lending Division as Supplementary Publication No. SUP 32430 (18 pp.). Copies may be obtained through The Executive Secretary, International Union of Crystallography, 13 White Friars, Chester CH1 1NZ, England.

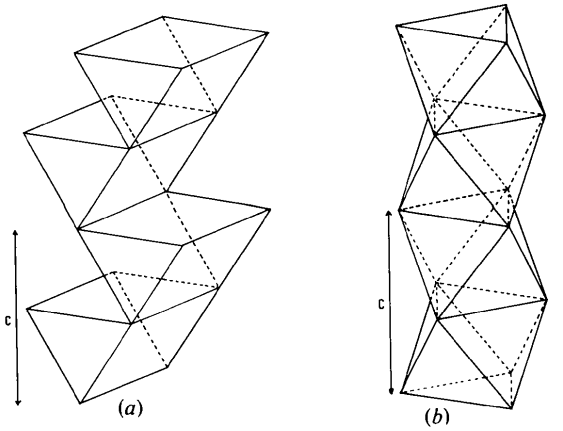

Fig. 1. (*a*) The linkage pattern of the trigonal prisms in the $M1$ chains. (*b*) The linkage pattern of the octahedra (or trigonal antiprisms) in the $M3$ chains.

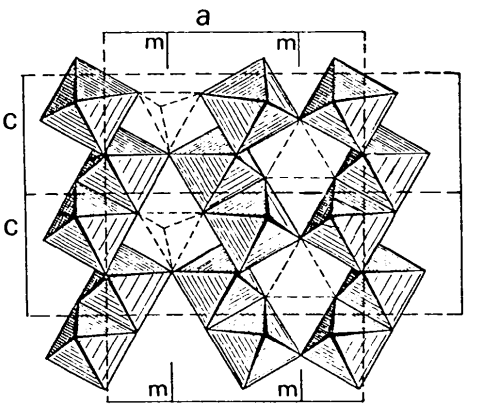

Fig. 2. The linkage pattern of the distorted octahedra in the [010] projection of the $M2$ layer.

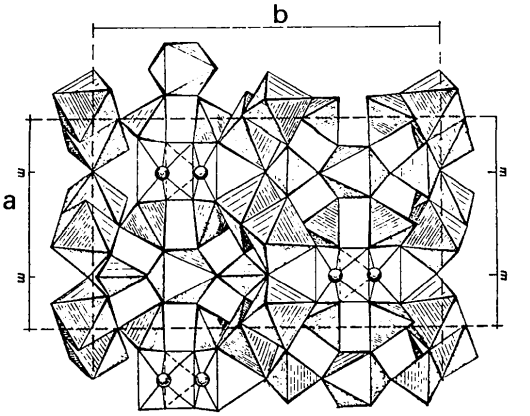

Fig. 3. The [001] projection of the structure of $Li_2Ni_2Mo_3O_{12}$.

Table 2. *Interatomic distances* (Å) *and bond angles* (°) *within the coordination polyhedra with the standard deviations given in parentheses*

Multiplicity is indicated in parentheses after the value.

Interatomic distances

Mo(1)–O(2)	1·764 (6)		*M*2–O(1′)	2·111 (3)	
–O(7)	1·780 (4)	(×2)	–O(5)	2·039 (4)	
–O(1)	1·795 (6)		–O(6)	2·055 (4)	
Average	1·780		–O(7)	2·134 (4)	
			–O(6′)	2·060 (4)	
Mo(2)–O(4)	1·741 (5)		–O(7′)	2·070 (4)	
–O(3)	1·771 (4)		Average	2·078	
–O(5)	1·774 (4)				
–O(6)	1·801 (4)		*M*3–O(2′)	2·090 (6)	
Average	1·772		–O(3‴)	2·045 (4)	(×2)
			–O(3)	2·025 (4)	(×2)
*M*1–O(4)	2·188 (18)	(×2)	–O(2)	2·112 (6)	
–O(5)	2·093 (15)	(×2)	Average	2·057	
–O(4′)	2·240 (16)	(×2)			
Average	2·174				

Interatomic angles

O(7)–Mo(1)–O(2)	109·04 (24)	(×2)
O(7)–Mo(1)–O(1)	109·49 (24)	(×2)
O(2)–Mo(1)–O(1)	114·62 (28)	
O(7)–Mo(1)–O(7″)	104·70 (19)	
Average	109·40	
O(3)–Mo(2)–O(5)	113·15 (20)	
O(4)–Mo(2)–O(3)	110·27 (21)	
O(3)–Mo(2)–O(6)	108·94 (19)	
O(4)–Mo(2)–O(6)	105·08 (21)	
O(5)–Mo(2)–O(6)	108·83 (20)	
O(5)–Mo(2)–O(4)	110·24 (21)	
Average	109·42	
O(5)–Li(1)–O(4)	91·17 (34)	(×2)
O(5)–Li(1)–O(4′)	81·30 (45)	(×2)
O(5)–Li(1)–O(5′)	85·69 (76)	
O(4)–Li(1)–O(4′)	79·82 (43)	(×2)
O(4)–Li(1)–O(4‴)	74·77 (72)	
O(4′)–Li(1)–O(4″)	72·76 (61)	
Average	81·98	
O(5)–Ni(2)–O(1′)	99·53 (15)	
O(5)–Ni(2)–O(7′)	90·74 (17)	
O(5)–Ni(2)–O(6)	97·43 (17)	
O(5)–Ni(2)–O(7)	86·04 (17)	
O(6′)–Ni(2)–O(7′)	87·01 (17)	
O(6′)–Ni(2)–O(1′)	86·48 (15)	
O(6′)–Ni(2)–O(7)	87·95 (17)	
O(6′)–Ni(2)–O(6)	83·70 (17)	
O(7)–Ni(2)–O(7′)	84·71 (17)	
O(7)–Ni(2)–O(6)	84·73 (17)	
O(1′)–Ni(2)–O(6)	94·88 (15)	
O(1′)–Ni(2)–O(7′)	94·76 (15)	
Average	89·83	
O(3)–Ni(3)–O(2′)	85·66 (21)	(×2)
O(3)–Ni(3)–O(3′)	84·92 (18)	
O(3)–Ni(3)–O(2)	93·11 (21)	(×2)
O(3)–Ni(3)–O(3‴)	94·57 (17)	(×2)
O(2)–Ni(3)–O(3‴)	86·74 (21)	(×2)
O(2′)–Ni(3)–O(3‴)	94·48 (21)	(×2)
O(3″)–Ni(3)–O(3‴)	85·95 (18)	
Average	90·00	

one corner with two *M*2 distorted octahedra, one corner with two *M*1 trigonal prisms and one corner with an *M*1 and an *M*2 polyhedron. Fig. 3 is a (001) projection of the structure. The observed pseudohexagonal symmetry of the crystals in the (*hk*0) precession photograph (Ozima & Zoltai, 1976) can be easily explained by the trigonal symmetry of the *M*3 octahedral chains and the arrangement of the Mo tetrahedra around these chains.

The interatomic distances and angles are given in Table 2. The average Mo–O distances in the *T*1 and *T*2 tetrahedra are 1·780 and 1·772 Å respectively, and their weighted average is 1·774 Å. These correspond reasonably well to the average Mo–O distances of 1·770 Å in $NaCo_{2.31}Mo_3O_{12}$ (Ibers & Smith, 1964), or 1·779 Å in $Li_3FeMo_3O_{12}$ and 1·773 Å in $Li_2Fe_2Mo_3O_{12}$ (Klevtsova & Magarill, 1971) and of 1·758 Å in $Cu_4Mo_3O_{12}$ (Katz *et al.*, 1971). The average (Ni,Li)–O distances in *M*1, *M*2 and *M*3 polyhedra are respectively 2·174, 2·078, and 2·057 Å. Their overall weighted average is 2·097 Å, which is within the range of expected bond lengths.

Systematics of the structure type

The crystal structures of these molybdates may be described and analysed as filled derivatives of a close-packed structure. That is, the O^{2-} ions are in close-packed sites and some voids between them are occupied by cations. In the well-known and common close-packed derivative structures, the anions are in

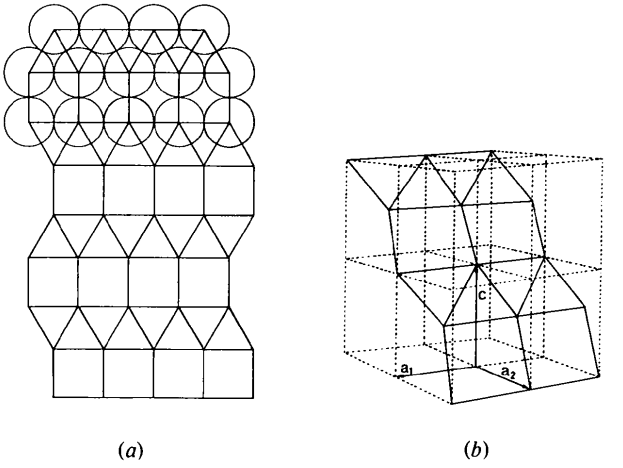

(*a*) (*b*)

Fig. 4. (*a*) The square-triangular close-packed sheet. For the simplicity of illustration atoms are not shown in the lower portion of this and subsequent diagrams. (*b*) A corrugated version of this close-packed sheet is in the (011) plane of the familiar hexagonal close-packed structure. The h.c.p. structure is illustrated by the outline of eight unit cells.

hexagonal or tetragonal close-packed sheets which are stacked in various sequences to produce cubic or hexagonal close-packed and tetragonal, rhombohedral or cubic body-centred close-packed structures. The close-packed sheets in these molybdates are neither hexagonal nor tetragonal, but are combinations of both triangular and square nets.

One of the two basic types of triangular-square nets, from which these molybdate structures can be derived, is the No. 9 regular net of Wells (1952) or the equivalent $3^3.4^2$ tessellation of Frank & Kasper (1959). This net, or close-packed sheet, is illustrated in Fig. 4(*a*). It should be noted that the same net, with minor corrugation, is present in the (011) plane of the common hexagonal close-packed derivative, or NiAs structure, as illustrated in Fig. 4(*b*). That is, the hexagonal close-packed structure can be interpreted either as an *AB* stacking of the hexagonal close-packed sheet or as a stacking of the triangular-square sheet, as shown in Fig. 5(*a*) and (*b*). Of course, the former is simpler and more meaningful as it relates this structure to other close-packed structures obtained by different stacking sequences of the same hexagonal sheet. However, the triangular-square sheet may also be stacked in a different fashion and produce other close-packed structures which no longer resemble the NiAs structure. An example of this is the structure of Er_3GaS_6 (Jaulmes & Laruelle, 1973), illustrated in Fig. 5(*c*). The voids created by this stacking no longer possess sixfold coordination, as in the hexagonal close-packed structure, but have four- and sevenfold coordination instead.

There are a number of other variations of this triangular-square sheet that yield different coordination polyhedra. While in the basic sheet there are alternating rows of single-width triangles and squares, in the malachite structure there are double rows of triangles alternating with single rows of squares (Fig. 6*a*). This sheet is called the *R*-layer by Lima-de-Faria & Figueiredo (1976). In the alloy structure of Pd_5B_2 (Stenberg, 1961) there are triple rows of triangles and double rows of squares (Fig. 6*b*).

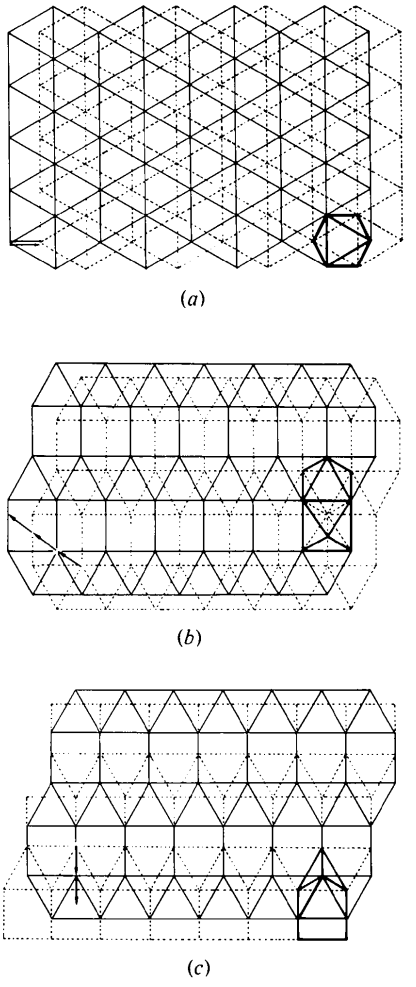

Fig. 5. (*a*) The *AB* stacking of the hexagonal close-packed sheet in the (001) plane of the h.c.p. structure. An octahedral void located between six close-packed atoms is illustrated in the lower right-hand corner. The stagger vectors are shown in the lower left-hand corner. (*b*) The stacking of the corrugated square-triangular sheet in the (011) plane of the same structure. The corrugation of the sheets is demonstrated by the shorter vertical sides of the squares. Two face-sharing, and apparently different, octahedral voids are illustrated. These two voids are actually identical because of the corrugation of the close-packed sheets. The stagger vectors of the stacking order are shown in the lower left-hand corner. (*c*) The same square-triangular sheets of sulphur stacked differently in Er_3GaS_6. The voids occupied by Er are trigonal prisms with an additional seventh bond, and those occupied by Ga are tetrahedra, which share a common face, as illustrated in the lower right-hand portion of the diagram. The stagger vectors are also shown.

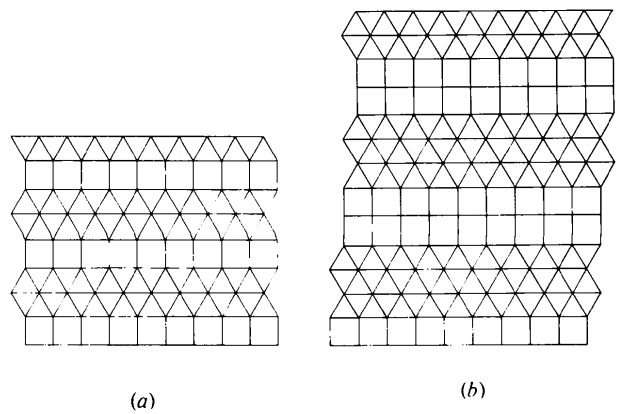

Fig. 6. (*a*) The modified square-triangular close-packed sheet of oxygens in the crystal structure of malachite. This is Lima-de-Faria's '*R*' layer type. (*b*) The modified square-triangular close-packed sheet of Pd in the structure of B_2Pd_5.

In our $M(1\text{–}3)_4Mo_3O_{12}$ structure type the basic triangular-square is broken into bands across the rows of triangles and squares. The bands are three squares and six triangles wide. The sheet is reconstituted with additional triangles between the bands. There is a small misregistry between the original bands. That misregistry is absorbed by the distortion of one of the connecting triangles as shown in Fig. 7(*a*). If the distance between the O atoms is taken as unity, the lengths of the three sides of this distorted triangle are: $\sqrt{(13/3 - \sqrt{12})} = 0{\cdot}932$, 1, $\sqrt{(7/3 - \sqrt{4/3})} = 1{\cdot}086$ and the three angles are (opposite to the sides given above): 52·91, 58·83, 68·26°. The unit mesh of this sheet is orthogonal (Fig. 7*b*) with unit translations **a** and **b**. If another identical layer is stacked on top of the first with an **a**/2 + **b**/2 displacement a variety of voids is created. The most regular of these voids are four- and sixfold coordinated, and are the prototypes of our $T1$, $T2$, $M1$, $M2$ and $M3$ polyhedra. The ideal close-packed structure, and the shape and the arrangements of the occupied voids are illustrated in Fig. 8. The dimensions of the voids are listed in Table 3 in terms of relative values with respect to O whose diameter is taken as unity.

In this regular close-packed structure, the dimensions and the symmetries of the voids are relatively inflexible as the O atoms are tightly packed and have almost no room available for displacement. However, the *close-packed* structure can be opened up by uniformly increasing the O–O distances and thus retain the symmetry and the pattern of the close-packed structure. In that *open-packed* structure the O atoms are no longer in contact and the dimensions of the voids are increased. The cation–O distances in the close-packed structure [for O^{III} radius equal to 1·28 Å, after Whittaker & Muntus (1970)] are: $T1 = T2$ 1·70, $M1$ 1·93, $M2 = M3$ 1·81 Å.

The reconstructed values of the same bond lengths, for example, in the open-packed structures of $Li_2Ni_2Mo_3O_{12}$ and $NaCo_{2.31}Mo_3O_{12}$ are respectively: $T1 = T2$ 1·87, $M1$ 2·12, $M2 = M3$ 2·00 and $T1 = T2$ 1·93, $M1$ 2·19, $M2 = M3$ 2·06 Å.

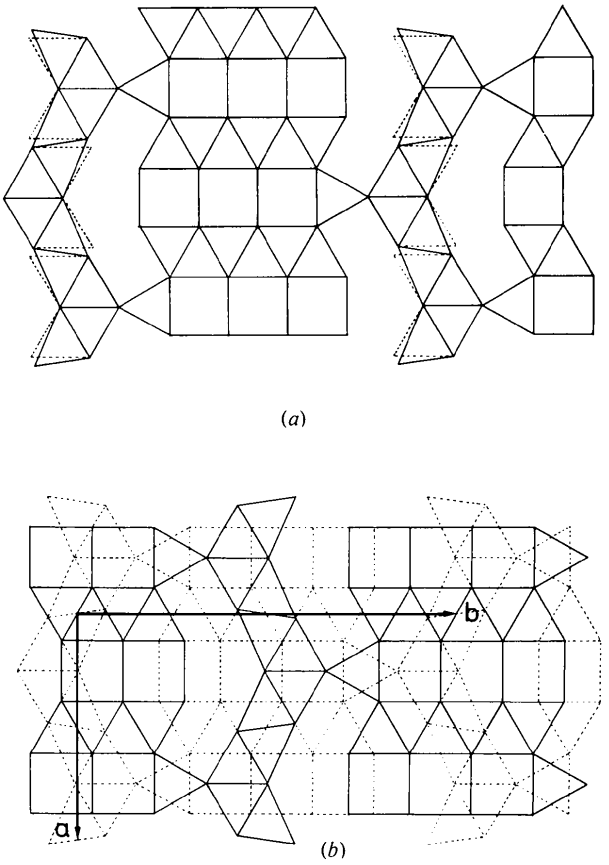

Fig. 7. (*a*) The modified square-triangular close-packed sheet in the $M(1\text{–}3)_4Mo_3O_{12}$. Three-squares-wide bands of the square-triangular sheet are connected by chains of triangles. The undistorted triangles are shown with dashed lines. (*b*) The stacking of two oxygen sheets and the location of the unit translations **a** and **b**.

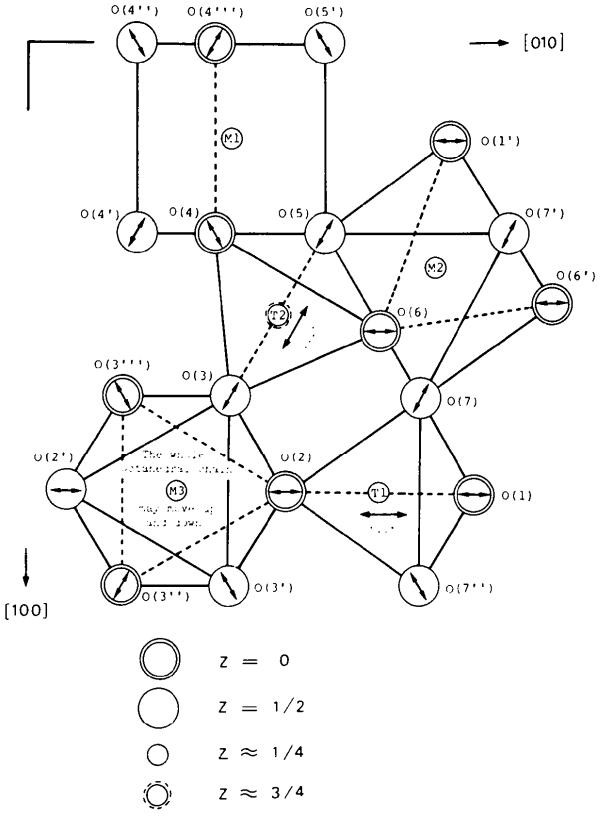

Fig. 8. Illustration of the various coordination polyhedra in the ideal $M(1\text{–}3)_4Mo_3O_{12}$ structure. The point of intersection of the [100] and [010] directions is approximately at $x = 1/8$, $y = 1/8$. Double-headed arrows in oxygens indicate the directions of oxygen displacement for adjusting for different cations in the voids. (The superscripts of oxygen numbers do not necessarily coincide with those in Table 2.)

Table 3. *Bond lengths, angles and edge length of coordination polyhedra in the ideal* $M(1–3)_4Mo_3O_{12}$ *structure*

Unit length equals O–O distance in the close-packed sheet.

Polyhedron	Edge		Edge length	*M*–O*	*M*–O*	Angle
*M*1	O(4)–O(4′)		$\sqrt{(2-\sqrt{\frac{4}{3}})}$	$\sqrt{(1-\sqrt{\frac{3}{16}})}$	$\sqrt{(1-\sqrt{\frac{3}{16}})}$	75·25°
	(4′)	(5)	1	$\sqrt{(1-\sqrt{\frac{3}{16}})}$	$\sqrt{(1-\sqrt{\frac{3}{16}})}$	83·21
	(4)	(5)				
	(5)	(5′)				
*M*2	(7)	(6)	$\sqrt{(2-\sqrt{\frac{4}{3}})}$	$\sqrt{(\frac{1}{2}+\sqrt{\frac{1}{48}})}$	$\sqrt{(\frac{5}{3}-\sqrt{\frac{27}{16}})}$	80·14
	(7)	(5)	1	$\sqrt{(\frac{1}{2}+\sqrt{\frac{1}{48}})}$	$\sqrt{(1-\sqrt{\frac{3}{16}})}$	79·93
	(1′)	(6′)				
	(7)	(6′)	$\sqrt{(2-\sqrt{\frac{1}{3}})}$	$\sqrt{(\frac{1}{2}+\sqrt{\frac{1}{48}})}$	$\sqrt{(1-\sqrt{\frac{3}{16}})}$	100·07
	(1′)	(5)				
	(7)	(7′)	1	$\sqrt{(\frac{1}{2}+\sqrt{\frac{1}{48}})}$	$\sqrt{(\frac{1}{2}-\sqrt{\frac{1}{48}})}$	90·00
	(6)	(5)	1	$\sqrt{(\frac{5}{3}-\sqrt{\frac{27}{16}})}$	$\sqrt{(1-\sqrt{\frac{3}{16}})}$	94·11
	(6)	(6′)	$\sqrt{(\frac{13}{3}-\sqrt{12})}$	$\sqrt{(\frac{5}{3}-\sqrt{\frac{27}{16}})}$	$\sqrt{(1-\sqrt{\frac{3}{16}})}$	85·89
	(6)	(1′)	$\sqrt{(2\frac{1}{3}-\sqrt{\frac{4}{3}})}$	$\sqrt{(\frac{5}{3}-\sqrt{\frac{27}{16}})}$	$\sqrt{(\frac{1}{2}+\sqrt{\frac{1}{48}})}$	99·87
	(5)	(7′)	1	$\sqrt{(1-\sqrt{\frac{3}{16}})}$	$\sqrt{(\frac{1}{2}-\sqrt{\frac{1}{48}})}$	94·94
	(6)	(7′)	$\sqrt{(2-\sqrt{\frac{4}{3}})}$	$\sqrt{(1-\sqrt{\frac{3}{16}})}$	$\sqrt{(\frac{1}{2}-\sqrt{\frac{1}{48}})}$	85·06
	(7′)	(1)	1	$\sqrt{(\frac{1}{2}-\sqrt{\frac{1}{48}})}$	$\sqrt{(\frac{1}{2}+\sqrt{\frac{1}{48}})}$	90·00
*M*3	(3)	(2)	1	$\sqrt{\frac{1}{2}}$	$\sqrt{\frac{1}{2}}$	90
T†	(7)	(2)	$\sqrt{(2-\sqrt{\frac{1}{3}})}$	$\sqrt{(\frac{21}{32}-\sqrt{\frac{3}{64}})}$	$\sqrt{(\frac{31}{32}-\sqrt{\frac{3}{64}})}$	128·14
	(2)	(1)	1	$\sqrt{(\frac{21}{32}-\sqrt{\frac{3}{64}})}$	$\sqrt{(\frac{21}{32}-\sqrt{\frac{3}{64}})}$	97·98

* *M*–O or *T*–O bond lengths are given in order of oxygens listed in the 'edge' column.

† *T*1 is identical with *T*2 in the ideal close-packed structure.

The O atoms in the open-packed structures have significantly more room available for displacement than in the equivalent close-packed structure, as there is more space between the O atoms. Consequently, the symmetries and the dimensions of the voids can be modified by small displacements of the O atoms in order to accept a limited variety of cations in the voids. In the Li, Ni, and Na, Co molybdates cited above the changes in some cation–anion distances may be as much as 25–30%.

As the O in these structures is three-coordinated, the displacement of any one O will modify both the bonding symmetries and the dimensions of three polyhedra, simultaneously. That is, the increase or decrease in the dimension and the change in the bond symmetry of one polyhedron causes coordinated modifications in two other polyhedra. The general pattern and symmetry of the structure is retained if the O displacements are limited to vertical movements and to those horizontal shifts which are indicated by arrows in Fig. 8. The patterns of coordinated O displacements, and of consequent changes in polyhedral dimensions and symmetries is complex. Although the derivation of a quantitative systematics for different sizes of cations (by neglecting other than dimensional characteristics of atoms) is feasible, only some qualitative observations will be offered in this paper.

The height of the polyhedral layers, or half of the **c** unit translation, is determined primarily by two factors: the shortening of the shared edges and the sizes of the cations occupying the three sixfold voids. The shortening of the shared edges of polyhedra is observed in many different crystal structures, especially in layered structures. An additional shortening (or expansion) of the horizontal edges, including unshared edges, can come through the adjustment of polyhedral heights. That is, if the heights of the *M*1, *M*2 and *M*3 polyhedra due to different cations occupying these sites are not the same, a common height can be obtained by the horizontal shift of the appropriate O atoms. These shifts are equivalent to additional shortening (or expansion) of the horizontal edges. For example, in the unadjusted open-packed structure of $NaCo_{2\cdot31}Mo_3O_{12}$ the height of the *M*1 polyhedron is a little higher (2·546 Å) than that of the *M*2 and *M*3 polyhedra (2·491 and 2·437 Å respectively) because of the large size of the Na cation. In $Li_2Ni_2Mo_3O_{12}$ the height of *M*1 (2·356 Å) in the unadjusted open-packed structure is lower than that of *M*2 and *M*3 (2·382 and 2·361 Å, respectively). The height of the layers in both of the observed structures is larger than that in their reconstructed open-packed structure, because of the normal shortening of the shared edges. However, that shortening is more extensive in the $Li_2Ni_2Mo_3O_{12}$ structure (by 9·6% of the other edges) than in the $NaCo_{2\cdot31}Mo_3O_{12}$ structure (by 5·2%), as the height of the Li polyhedron had to be *increased* and that of the Na polyhedron *decreased*. The same trend is demonstrated by the relative length of the unshared prismatic edge. That edge is shorter than the other unshared edges in the Li, Ni structure (by 2·3%), and is longer in the Na, Co structure (by 4·9%). The observations indicate that the shortening of the shared edges is more extensive in the Li, Ni, and less extensive in the Na, Co structure than should be due to sharing alone.

The tetrahedral voids in this structure are sensitive to the horizontal dimensions of the other voids. The column of *M*3 octahedra is in the centre of the channel of the *M*1–*M*2 polyhedral network and is connected to that network by the tetrahedra. In the ideal close or open-packed structure, the tetrahedra are oriented so that two edges are horizontal, as shown in Fig. 8. However, if the channels are small or the dimensions of the *M*3 octahedra are larger than ideal, tetrahedra will adjust by tilting and by distortion. In the case of the Li, Ni molybdate, for example, the tilt of the *T*1 tetrahedron is 20·8° and the tetrahedral angles are distorted to values ranging between 104·7 and 114·6°.

Although this structure type is capable of adjustment to various sizes of cations, the ranges of possible adjustments are relatively limited and the consequent distortions, especially of the tetrahedra, are relatively extensive. Consequently, the number of possible compositions for this structure type is expected to be limited.

The calculations were performed on the FACOM 230-48 Computer at the Institute for Solid State Physics, University of Tokyo.

References

FRANK, F. C. & KASPER, J. S. (1959). *Acta Cryst.* **12**, 483–499.

IBERS, J. A. & SMITH, G. W. (1964). *Acta Cryst.* **17**, 190–197.

International Tables for X-ray Crystallography (1974). Vol. IV, pp. 72–83. Birmingham: Kynoch Press.

JAULMES, S. & LARUELLE, P. (1973). *Acta Cryst.* B**29**, 352–354.

KATZ, L., KASENALLY, A. & KIHLBORG, L. (1971). *Acta Cryst.* B**27**, 2071–2077.

KLEVTSOVA, R. F. & MAGARILL, S. A. (1971). *Sov. Phys. Crystallogr.* **15**, 611–615.

LIMA-DE-FARIA, J. & FIGUEIREDO, M. O. (1976). *J. Solid State Chem.* **16**, 7–20.

OZIMA, M. & ZOLTAI, T. (1976). *J. Cryst. Growth*, **34**, 301–303.

STENBERG, B. E. (1961). *Acta Chem. Scand.* **15**, 861–870.

TOKONAMI, M. (1965). *Acta Cryst.* **19**, 486.

WELLS, A. F. (1952). *The Third Dimension in Chemistry*, 2nd ed. Oxford: Clarendon Press.

WHITTAKER, E. J. W. & MUNTUS, R. (1970). *Geochim. Cosmochim. Acta*, **34**, 945–956.

Acta Cryst. (1977). B**33**, 2181–2188

The Structure of 1,1′-Diethyl-2,2′-cyanine Iodide, a Photographic Sensitizing Dye

BY KAZUMI NAKATSU, HIROSHI YOSHIOKA AND HIROAKI MORISHITA

Faculty of Science, Kwansei Gakuin University, Uegahara, Nishinomiya, Hyogo 662, *Japan*

(*Received* 9 *November* 1976; *accepted* 25 *December* 1976)

The crystal structure of the title compound, $(C_{23}H_{23}N_2)^+I^-$, a well known spectral sensitizing dye in silver halide photography, has been determined by single-crystal X-ray analysis. The compound crystallizes in the monoclinic space group $P2_1/c$, with four formula units in a cell of dimensions: a = 10·787 (3), b = 11·626 (2), c = 16·484 (3) Å, and β = 107·48 (3)°. The structure was refined by block-diagonal least-squares calculations to a conventional R of 0·032 for 2177 observed reflexions collected on an automatic diffractometer. The dye cation assumes a skewed conformation with approximate symmetry 2 (C_2); the dihedral angle between the roughly planar quinoline rings is 41°. In the crystals each quinoline ring of the dye cation is stacked in a face-to-face manner with adjacent cations to form a double linear array along [101]. The intense, sharp J absorption band observed on a powder sample is ascribable to the linear array. A charge-transfer interaction between the dye cation and the iodide anion is suggested to be present from an SCF–MO calculation on the dye cation; this is evidenced by the crystal structure.

Introduction

Many photographic sensitizing dyes exhibit striking spectral shifts on aggregation in solution and on the surfaces of silver halide grains, and are interesting from both practical and theoretical points of view. Various one- and two-dimensional packing models of the dyes in the aggregates have been proposed. The actual molecular arrangements in the aggregates, however, have not definitely been established. Since the crystalline state is a three-dimensional aggregate of the constituents, the crystal structures of the dyes, as reviewed by Smith (1974), can provide a reliable structural model for the aggregates.

Of particular interest is 1,1′-diethyl-2,2′-cyanine halide (Fig. 1, hereinafter DYE halide), which is a typical quinocyanine dye exhibiting red- and blue-shifted absorption bands on aggregation (West & Carroll, 1966, a review). The absorption spectrum of a very dilute aqueous solution of the DYE halide shows a maximum near 525 nm (called the M band) (see Fig. 7). On increasing the DYE concentration a new band appears at about 485 nm, and subsequently an intense, remarkably sharp band at 573 nm. These bands, named H and J bands, are ascribed to dimeric and polymeric aggregates, or H and J aggregates respectively. The J band is

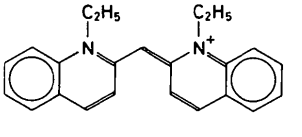

Fig. 1. Chemical structure of 1,1′-diethyl-2,2′-cyanine (DYE) iodide. This nomenclature is the most common (Brooker, 1966). Alternative names are: 1,1′-diethyl-2,2′-quinocyanine, *N,N′*-diethylpseudoisocyanine, bis(1-ethyl-2-quinoline)monomethine cyanine, *etc.*